ICSV13 - Vienna
The Thirteenth International Congress on Sound and Vibration
Vienna, Austria, July 2-6, 2006

VIBRATION ANALYSIS OF INITIALLY TWISTED SHELL TYPE BLADES SUBJECTED TO THERMAL LOADS

Youngjung Kee*[1], Deog-Kwan Kim[1], Seung-Ho Kim[1], Ji-Hwan Kim[2]

[1]Rotor System Department, Korea Aerospace Research Institute
45 Eoeun-Dong Yuseong-Gu, Daejeon, 305-806, Republic of Korea
[2]School of Mechanical & Aerospace Engineering, College of Engineering
Seoul National University, Seoul, 151-742, Republic of Korea
naltlguy@kari.re.kr (e-mail address of lead author)

Abstract

Nowadays, shell-type structures are widely used as a part of the turbo-machines. These structures have different curvatures, which are the main feature relative to the beam or plate models. Thus, shell models are preferable to beam or plate models because the shell models consider the effect of surface curvatures. The purpose of this study is to analyze the free vibration characteristics of a rotating blade subjected to the centrifugal force, Coriolis acceleration and thermal loads. In this study, general formulation is proposed to analyze the initially twisted rotating shell-type blades in thermal environment, and the finite element method is adopted for solving the governing equations.

INTRODUCTION

In aeronautical and aerospace engineering, rotating blades are the main structural members of turbo-machines. Because these blades must perform efficiently with high specific strength, they must undergo vibration analysis. Thus, the vibration analysis of turbo-machinery blades has been widely investigated, and has been part of the investigations in numerous publications.

Nowadays, shell-type structures are widely used as a part of the turbo-machines. These structures have different curvatures, which are the main feature relative to the beam or plate model. Thus, shell models are preferable to beam or plate models because those can't consider the effect of surface curvature. Leissa and his co-workers did extensive researches that greatly help in assessing the vibration characteristics of shell type turbo-machinery blades [1-4]. Those methods in references can be used for analyzing blades with relatively small double curvatures accurately, but are inadequate for blades with large curvatures and twists.

For decades, there have been considerable activities in the analysis of shell structures by the finite element method. Henry et al. [5] summarized the important literatures on shell finite elements that have been developed in decades. Ahmad et al. [6] introduced the concept of the continuum based degenerated shell element, and treated shells of arbitrary shapes without adopting complicated assumptions for specific shell theories. The popularity of this concept due to their simplicity in the formulation, many researchers has been developed and improved the behaviour of that element. The geometric and material nonlinear analysis of shells was extended by Ramm [7] and Bathe and Bolourchi [8]. Huang and Hinton [9] presented a new nine-node degenerated shell element, which adopts an enhanced interpolation to overcome the locking phenomenon. Recently, Lee and Han [10] investigated the free vibration of plates and shells by using the assumed natural strains.

The purpose of this study is to analyze the vibration characteristics of rotating shell-type blades subjected to the centrifugal force, Coriolis acceleration and thermal loads. In this study a general formulation is proposed to analyze the initially twisted rotating shell-type blades in thermal environment. The blade is assumed to be a moderately thick shell which includes the transverse shear deformation and rotary inertia, and is oriented arbitrarily about the axis of rotation to consider the effects of disk radius and setting angle. In the numerical study, the effects of the various parameters are investigated; initial twists, rotating speeds, disk radius and thermal boundary conditions.

FORMULATION

Basic Assumptions

In this study, we will use the assumptions as,

- A straight normal to the mid-surface before deformation remains straight after deformation, and the transverse shear deformation is considered.
- A stress component normal to the shell mid-surface is negligible.
- Thermo-mechanical properties of the blade are independent of the temperature, and the thickness temperature gradient of the blade is negligible.

Geometry and Deformation of Shell Element

The position vector $\mathbf{X}$ of a generic material point P in the undeformed configuration, and the unit nodal vectors and the coordinates adopted in this study are depicted in Figure 1. The position vector $\mathbf{X}$ can be expressed as

$$\mathbf{X} = \mathbf{X}_0 + z\,\mathbf{e}_3 \tag{1}$$

where $\mathbf{X}_0$ is the position vector of a point O on the shell midsurface and $\mathbf{e}_3$ the unit normal vector of the shell midsurface. Using the nondimensional coordinate ς with respect to the thickness t of the shell, Eq. (1) is changed as follows

$$\mathbf{X} = \mathbf{X}_0 + \varsigma\left(t/2\right)\mathbf{e}_3 \tag{2}$$

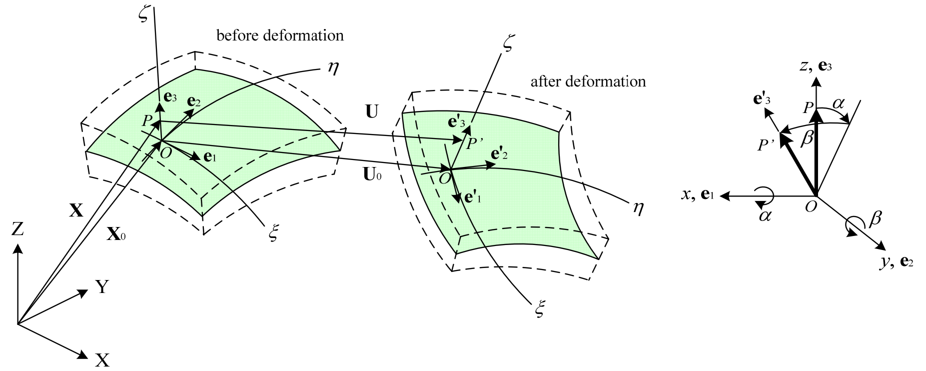

Figure 1－Kinematics of shell deformation

The line segment $\overline{OP}$ changes to $\overline{OP'}$, and then $z\mathbf{e}_3$ rotates $z\mathbf{e'}_3$ after deformation. Then the displacement vector $\mathbf{U}$ of a generic material point P can be written as

$$\mathbf{U} = \mathbf{U}_0 + \varsigma \mathbf{U}_\varsigma; \quad \mathbf{U}_\varsigma = t(\mathbf{e}_3^{'} - \mathbf{e}_3)/2 \tag{3}$$

In this study, we used the isoparametric nine-node element. Five degrees of freedom are defined at each nodal point corresponding to its three translational displacements u_0, v_0, w_0 and two rotational degrees of freedom α and β.

Thermal-Structural Interface

We assume that the heat conduction occurs in a rotating blade with velocity components (γ_x, γ_y), and no internal heat generation and radiation; hence the governing equation of steady state heat conduction can be derived as

$$k_x \frac{\partial^2 T}{\partial x^2} + k_y \frac{\partial^2 T}{\partial y^2} + k_z \frac{\partial^2 T}{\partial z^2} - \rho c_p \gamma_x \frac{\partial T}{\partial x} - \rho c_p \gamma_y \frac{\partial T}{\partial y} = 0 \tag{4}$$

The Galerkin weighted residual method is applied to the equation (4) to obtain the finite element equation. Then, one can derive the following equation in the form as

$$(\mathbf{K}_{cn} + \mathbf{K}_{cv})\mathbf{T} = \mathbf{P}_h \tag{5}$$

where $\mathbf{K}_{cn}$, $\mathbf{K}_{cv}$ and $\mathbf{P}_h$ denote the heat conductance matrix, heat convectivity matrix and the heat flux vector, respectively. In addition, the stress-strain relationship with respect to the global coordinate system can be written as

$$\boldsymbol{\sigma} = \mathbf{E}(\boldsymbol{\varepsilon} - \mathbf{T}\boldsymbol{\alpha}) \text{ or } \boldsymbol{\sigma} = \mathbf{E}(\boldsymbol{\varepsilon} - \boldsymbol{\varepsilon}_t) \tag{6}$$

in which $\boldsymbol{\sigma}$, $\mathbf{E}$, $\boldsymbol{\alpha}$, $\boldsymbol{\varepsilon}$ and $\boldsymbol{\varepsilon}_t$ are, respectively, the stress, material property matrix, thermal expansion coefficient vector, the total strain and the thermal strain vectors.

Governing Equation

The coordinate nodal values were used to interpolate the position and displacement vectors, and these vectors are expressed as follows

$$\mathbf{X} = \sum_{i=1}^{9} N_i [\mathbf{X}_0]_i + \varsigma \sum_{i=1}^{9} N_i \left[\frac{t}{2}\mathbf{e}_3\right]_i, \; \mathbf{U} = \sum_{i=1}^{9} N_i [\mathbf{U}_0]_i + \varsigma \sum_{i=1}^{9} N_i \left[\frac{t}{2}\mathbf{U}_\zeta\right]_i \tag{7}$$

The covariant displacement components in the natural coordinate system are obtained by projecting the displacement components expressed in the global Cartesian coordinate system onto the natural coordinate directions, which are expressed as

$$\mathbf{u}_\alpha = \frac{\partial x^i}{\partial \xi^\alpha}\mathbf{u}_i \tag{8}$$

where repeated indices denote the summation ($i = 1,2,3$, $\alpha = \xi, \eta, \varsigma$). Equation (9) can also be rewritten in a matrix form as

$$\begin{Bmatrix} u_\xi \\ u_\eta \\ u_\varsigma \end{Bmatrix} = \begin{bmatrix} x_{,\xi} & y_{,\xi} & z_{,\xi} \\ x_{,\eta} & y_{,\eta} & z_{,\eta} \\ x_{,\varsigma} & y_{,\varsigma} & z_{,\varsigma} \end{bmatrix} \begin{Bmatrix} u \\ v \\ w \end{Bmatrix} = \mathbf{J}\lfloor u \;\; v \;\; w \rfloor^T \tag{9}$$

With rotational motion $\mathbf{\Omega}$, the velocity vector of any arbitrary point of the blade may be written as

$$\mathbf{v} = d\mathbf{r}/dt + \mathbf{\Omega} \times \mathbf{r} \tag{10}$$

To derive the governing equation of motion, Hamilton's principle is used as

$$\int_{t_0}^{t_1} (\delta T - \delta U)\, dt = 0 \tag{11}$$

The variation on the strain energy U and kinetic energy T can be written as

$$\delta U = \int_V \left[\delta\varepsilon_{xx} E \varepsilon_{xx} + \delta\varepsilon_{yy} E \varepsilon_{yy} + \delta\gamma_{xy} G \gamma_{xy} + \delta\gamma_{yz} G \gamma_{yz} + \delta\gamma_{xz} G \gamma_{xz}\right] dV \tag{12}$$

$$\delta T = -\int_V \rho \{\bar{P}_u\, \delta u + \bar{P}_v\, \delta v + \bar{P}_w\, \delta w\}\, dV \tag{13}$$

Hence the governing equation is derived as

$$\mathbf{M}\ddot{\mathbf{q}} + \mathbf{C}\dot{\mathbf{q}} + \left(\mathbf{K}_l + \mathbf{K}_g + \mathbf{K}_{cf} + \mathbf{K}_t\right)\mathbf{q} = \mathbf{F}_{cf} \tag{14}$$

where $\mathbf{M}$, $\mathbf{C}$, $\mathbf{K}_l$, $\mathbf{K}_g$ and $\mathbf{K}_t$ are the mass matrix, the Coriolis matrix, the linear stiffness matrix, the geometric stiffness matrix and thermal stiffness matrix, respectively. In addition, $\mathbf{K}_{cf}$ and $\mathbf{F}_{cf}$ are the stiffness matrix and the force vector due to the centrifugal force.

For the dynamic analysis, the solution of equation (14) is separated to the static and time dependent terms. Then the displacement vector $\mathbf{q}$ may be expressed as $\mathbf{q} = \mathbf{q}_s + \boldsymbol{\delta}(t)$, where $\mathbf{q}_s$ and $\boldsymbol{\delta}(t)$ denote the static solution and a small time dependent perturbation about the static equilibrium state, respectively. Thus, we can obtain the perturbed equation as follows:

$$\mathbf{M}\ddot{\boldsymbol{\delta}} + \mathbf{C}\dot{\boldsymbol{\delta}} + \left(\mathbf{K}_l + \mathbf{K}_g + \mathbf{K}_{cf} + \mathbf{K}_t\right)\boldsymbol{\delta} = \mathbf{0} \tag{15}$$

To derive the eigenvalue problem, equation (15) is transformed into the following form:

$$\mathbf{A}\mathbf{g} - \mathbf{B}\dot{\mathbf{g}} = \mathbf{0} \tag{16}$$

where $\mathbf{A} = \begin{bmatrix} \mathbf{M} & \mathbf{0} \\ \mathbf{0} & \mathbf{K} \end{bmatrix}$, $\mathbf{B} = \begin{bmatrix} \mathbf{0} & \mathbf{M} \\ -\mathbf{M} & -\mathbf{C} \end{bmatrix}$ and $\mathbf{g} = \lfloor \dot{\boldsymbol{\delta}} \;\; \boldsymbol{\delta} \rfloor^T$.

Table 1 — Natural frequencies (Hz) of the open cylindrical shell-type blade

Mode Number	Present	Ref.[2]	Ref.[11]	
		Analytic Sol.	Experiment	FEM
1	85.4	85.9	85.6	86.6
2	139.7	137.8	134.5	139.2
3	251.8	248.6	259.0	251.3
4	347.7	342.9	351.0	348.6
5	391.6	378.4	395.0	393.4

NUMERICAL RESULTS

Validation of the Model

The shell element has been used for the analysis of the vibration characteristics of initially twisted shell type blades. The blade is assumed to be a moderately thick shell which includes the transverse shear deformation and rotary inertia, and a shear correction factor 5/6 is used in the analysis.
Table 1 shows the quantative comparisons of lowest five natural frequencies of a non-rotating steel fan blade. The natural frequencies obtained by the present shell elements are compared with the results in Ref. [2. 11], and agree well with those of reference data. Figure 2 shows the non-dimensional frequency parameters of twisted plate-type blade models, and the present model is same as in Ref. [12]. The symbols 1B, 2B denote spanwise bending frequencies, 1T the torsional frequency, 1EB the edgewise bending frequency and 1CB the chordwise bending frequency. The present results display quite good agreements with the reference data.
To confirm that the numerical procedure is practical for analyzing the thermal-structural interaction, the present results are compared with those of the analytic calculation in Ref. [13]. The quantative comparisons of temperature distribution of a plate that was subjected to the Dirichlet boundary conditions are shown in Figure 3. The results between the previous work and the present data are almost the same.

Application of the Model

Figure 4 depicts the configuration of a rotating shell-type blade model for the present study. Dimensionless parameter Ω denotes the ratio of rotating speed with respect to the fundamental natural frequency of the non-rotating blade. In addition, the local coordinate system (x, y, z) has the offset from the global Cartesian coordinate system (X, Y, Z) by translation (h_i, h_i, h_k) and rotation $(\theta_i, \theta_j, \theta_k)$.

Table 2 − Material properties of rotating blade for numerical study

Properties	Values	Properties	Values
Elastic Modulus	E=200GPa	Chord Length	a(tip), b(root)=30.5cm
Shear Modulus	$G=E/2(1+\upsilon)$	Blade Radius	$R_y=2a$
Density	$\rho=7{,}680 Kg/m^3$	Blade Thickness	t=a/100
Poisson's Ratio	$\upsilon=0.3$		

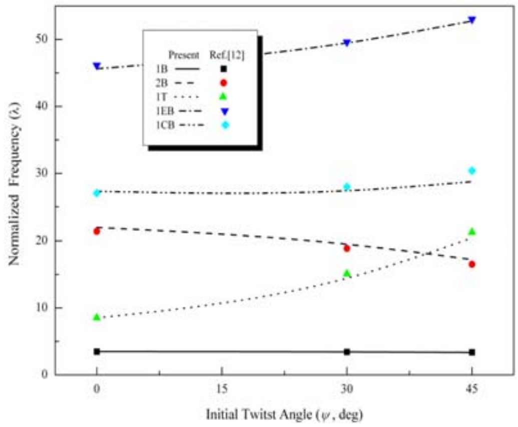

Figure 2 — Normalized frequency parameters of the plate-type blade ($\lambda = \omega a^2 \sqrt{\rho h / D}$)

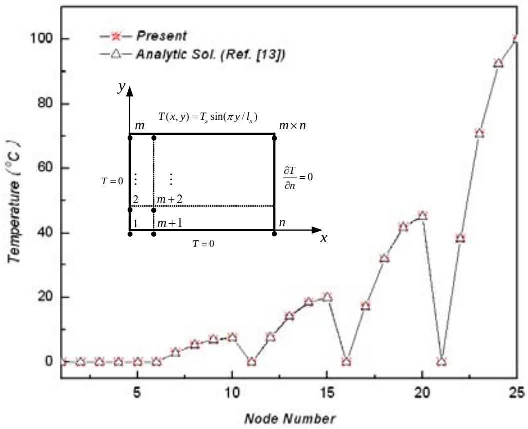

Figure 3 — Comparison of temperature distribution (m,n=5, T_s=100 ℃, L_x=5)

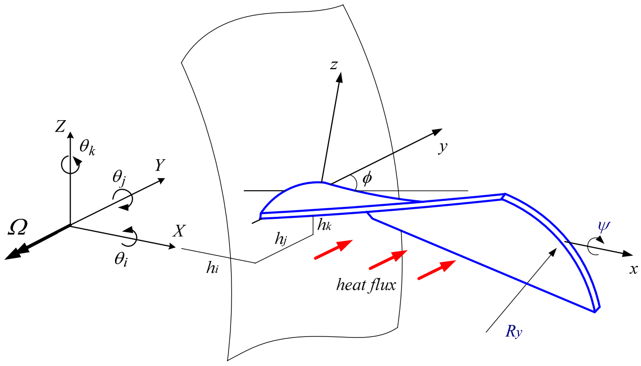

Figure 4 — Geometry of a initially twisted shell-type blade model attached to a rigid hub

Figure 5 shows the natural frequencies of rotating blade with the initial twist ψ. Dimensionless rotating speed Ω varies from 0.0 to 2.0 and is defined as $\Omega = \omega / \omega_{NR}$. This figure shows that as increase in the rotating speed of a blade, the higher natural frequencies are acquired. As is well known, this behavior means that the blade was stiffened by the blade's rotation and can resist further bending and twisting deformation. In this figure, as the initial twists are increased, the bending frequencies of non-rotating blade ($\Omega = 0$) tend to decrease, gradually. As the blade starts to rotate, the increase rates of bending frequencies are changed dramatically. In addition, the torsional frequencies are increased with the initial twist and rotating speed.

Most turbo-machinery blades are operated in a thermal environment. Thus, we must consider the elastic deformations of the blade due to the thermal disturbances. The following material properties of an aluminum alloy 2024 6-T were used in the numerical study.

Table 3 − Material properties for thermal analysis

Properties	Values	Properties	Values
Elastic Modulus	E=75.0GPa	Conductivity	k=177W/m·K
Density	ρ=2,770Kg/m^3	Specific Heat	C_p=875J/kg·K
Poisson's Ratio	υ=0.33	Thermal Exp. Coef.	$\alpha=73\times10^{-6}$/K

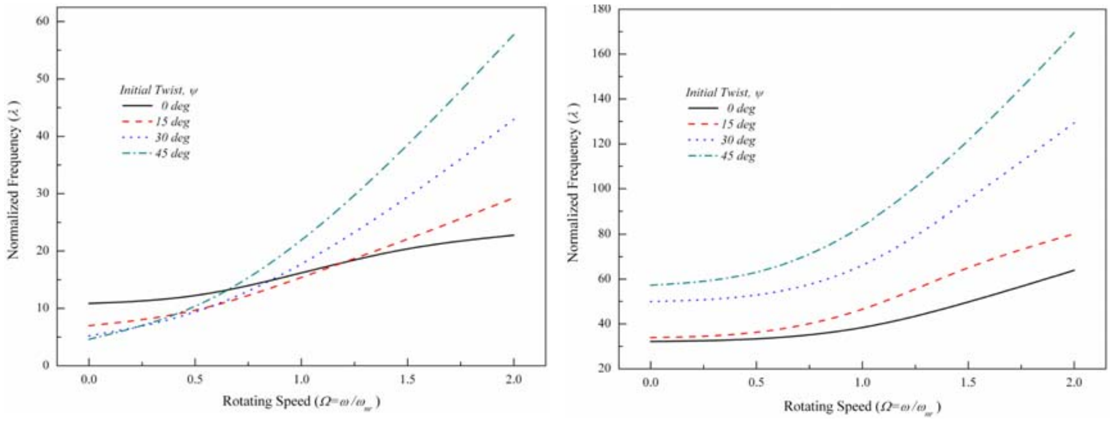

(a) 1st Bending mode *(b) 1st Torsional mode*

Figure 5－Frequency variations of a rotating blade with the initial twist

The rotating blade is often exposed to heat flux. In this case, one must consider the velocity components because of the convectional effects. Figure 6 shows the variations of natural frequencies of a rotating blade subjected to thermal constraints. The blade base is maintained at a constant temperature (300K), and the heat flux is applied to the leading edge of blade. From the results, the calculated normalized frequencies are falling down with surrounding temperature, gradually. This is because the temperature variation weakens the stiffness of the blade, thus the lower frequencies are generated. Figure 7 displays the variation in the calculated natural frequencies with different disk radius. Dimensionless parameter l_r which varies from 0.5 to 2.0 implies the ratio of disk radius with respect to the blade chord length and is defined as $l_r=h_i/a$. In general, the convectional effects depend on the velocity components (γ_x, γ_y), and those velocity components are linearly proportional to the disk radius. Thus, lower frequencies are expected when the disk radius increases. However, numerical results indicate that the disk radius seems sensitive to the natural frequencies in this case. This behavior reveals that the convectional thermal effects with the velocity components are smaller than the inplane centrifugal hardening effects induced by blade's rotation.

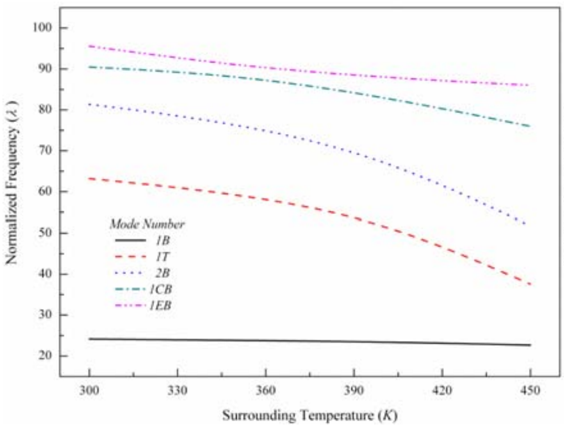

Figure 6－ Frequency variations upon the surrounding temperature

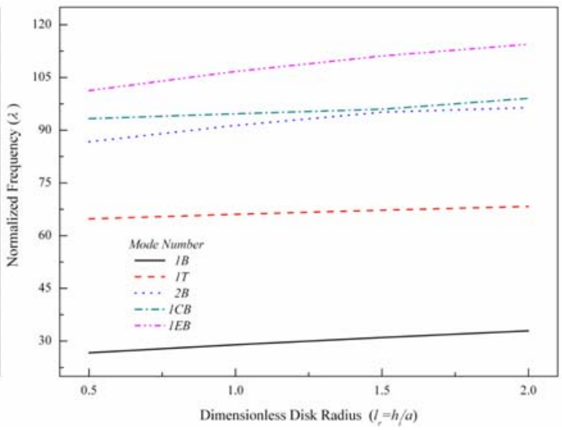

Figure 7－ Frequency variations as a function function of the disk radius (q=1,000W/m^2)

CONCLUSIONS

In this study, a general formulation is proposed to analyze the vibration characteristics of initially twisted rotating shell-type blades, and the finite element method is adopted for solving the governing equations. The effects of the various parameters were investigated, such as initial twist, rotating speed, disk radius and thermal constraints. For an initially twisted non-rotating blade, the bending frequencies tended to decrease, whereas the torsional frequencies are increased with the initial twist. As the blade starts to rotate, the higher natural frequencies are acquired. The centrifugal force due to the blade's rotational motion affects vibration characteristics of blade, dominantly. As the initial twisting angles are increased, the bending frequencies tend to decrease gradually, but the increase rates of bending frequencies are changed dramatically. In addition, the torsional frequencies are increased with the initial twist. The calculated normalized frequencies are falling down with surrounding temperature, and the disk radius seems more sensitive to the natural frequencies than the convectional thermal effects.

REFERENCES

[1] Leissa, A. W., Lee, J. K. and Huang, A. J., "Vibrations of cantilevered cylindrical shallow shells having rectangular planform", Journal of Sound and Vibration, Vol. 78(3), 1981, pp. 311-328.
[2] Leissa, A.W., Lee, J.K. and Wang, A.J., "Rotating blade vibration analysis using shells", Journal of Engineering for Power, Vol. 104, 1982, pp. 296-302.
[3] Leissa, A.W., Lee, J.K. and Huang, A.J., "Vibrations of cantilevered doubly-curved shallow shells", International Journal of Solids and Structures, Vol. 19(5), 1983, pp. 411-424.
[4] Leissa, A.W., Lee, J.K. and Huang, A.J., "Vibrations of twisted rotating blades", ASME Journal of Vibration, Acoustics, Stress and Reliability in Design, Vol. 106(2), 1984, pp. 251-257.
[5] Henry, T.Y., Masud, A. and Kapania, R.K., "A survey of recent shell finite elements", International Journal for Numerical Methods in Engineering, Vol. 47, 2000, pp. 101-127.
[6] Sohrabuddin Ahmad, Bruce M. Irons and O.C. Zienkiewicz, "Analysis of thick and thin shell structures by curved finite elements", International Journal for Numerical Methods in Engineering, 1970, Vol. 2, pp. 419-451
[7] E. Ramm, A plate/shell element for large deflections and rotations", in K.J. Bathe (ed.), *Formulations and Computational Algorithms in Finite Element Analysis*, MIT press, Cambridge, MA, 1977.
[8] K.B. Bathe and S. Bolourchi, "A geometric and material nonlinear plate and shell element", Computers & Structures, Vol. 11, 1980, pp. 23-48.
[9] H.C. Huang and E. Hinton, "A new nine node degenerated shell element with enhanced membrane and shear interpolation", International Journal for Numerical Methods in Engineering, Vol. 22, 1986, pp. 73-92.
[10] S.J. Lee and S.E. Han, "Free vibration analysis of plates and shells with a nine-node assumed natural degenerated shell element", Journal of Sound and Vibration, Vol. 241(4), 2001, pp. 605-633.
[11] M.D. Olson and G.M. Lindberg, "Dynamic analysis of shallow shells with a doubly curved triangular finite element", Journal of Sound and Vibration, Vol. 19(3), 1971, pp. 299-318.
[12] S. Mohamad Nabi and N. Ganesan, "Comparison of beam and plate theories for free vibration of metal matrix composite pre-twisted blades", Journal of Sound and Vibration, 1996, Vol. 189(2), pp. 149-160
[13] J.S. Carslaw and C. Jaegar, *Conduction of Heat in Solids*, Clarendon, Oxford, 1959, pp.177